Check for updates

Optics Letters

10-W-scale Kerr-lens mode-locked Yb:CALYO laser with sub-100-fs pulses

Wenlong Tian,[1] Rui Xu,[1] Li Zheng,[1] Xuan Tian,[1] Dacheng Zhang,[1,*] Xiaodong Xu,[2] Jiangfeng Zhu,[1,5] Jun Xu,[3] and Zhiyi Wei[4]

[1]School of Physics and Optoelectronic Engineering, Xidian University, Xi'an 710071, China
[2]Jiangsu Key Laboratory of Advanced Laser Materials and Devices, School of Physics and Electronic Engineering, Jiangsu Normal University, Xuzhou 221116, China
[3]School of Physics Science and Engineering, Tongji University, Shanghai 200092, China
[4]Beijing National Laboratory for Condensed Matter Physics and Institute of Physics, Chinese Academy of Sciences, Beijing 100190, China
[5]e-mail: jfzhu@xidian.edu.cn
*Corresponding author: dch.zhang@xidian.edu.cn

Received 8 January 2021; revised 27 January 2021; accepted 3 February 2021; posted 4 February 2021 (Doc. ID 419370); published 5 March 2021

We reported a high-power pure Kerr-lens mode-locked Yb:CALYO laser based on the dual-confocal cavity delivering sub-100-fs pulses. The output pulses at 81 MHz have an average power of 10.4 W and the pulse duration of 98 fs, corresponding to the peak power of 1.14 MW. This is, to the best of our knowledge, the highest average power ever reported for a Kerr-lens mode-locked Yb-bulk oscillator. Analysis of the dual-confocal cavity was also conducted, which indicates a way to achieve higher average power. We believe the result described in this Letter may pave a way to develop Kerr-lens mode-locked bulk lasers with much higher average power.

https://doi.org/10.1364/OL.419370

The generation of high-power ultrashort pulses has always been attractive to researchers due to its wide range of applications in scientific researches and industries [1,2]. With excellent thermal management, the thin-disk laser (TDL) is one of the most popular methods to generate high-power ultrashort pulses directly from the laser oscillator [3]. Average output power as high as 270 W [4] by Kerr-lens mode-locking (KLM) and up to 350 W [5] using a semiconductor saturable absorber mirror (SESAM) has been reported successfully. However, the pulse durations are typically several hundred femtoseconds due to the narrow emission bandwidth of the most widely used Yb:YAG thin disk. To obtain sub-100-fs pulses, the $Yb:Lu_2O_3$ and the Yb:CALGO thin disk have been employed in the past years. However, the average power was only 1.6 W for 35 fs pulse duration [6], 5.1 W for 62 fs pulse duration [7], and 21 W for 95 fs pulse duration [8]. In fact, this kind of level of average power does not need very high pump power whose thermal load is actually in the reachable margin of conventional Yb-bulk lasers. Considering the difficulty of the fabrication of a high-quality thin disk and the complexity of the pumping geometry, it is significant to develop high-power bulk lasers with short pulse duration.

As for the high-power ultrashort bulk lasers, there are more suitable gain media with both high thermal conductivity and wide spectral bandwidth, such as Yb:KGW [9], $Yb:CaF_2$ [10], $Yb:Lu_2O_3$ [6], Yb:YSO [11], Yb:CALGO [12], and Yb:CALYO [13]. With the help of a SESAM, several watt-level Yb-doped bulk lasers with sub-100-fs pulses have been demonstrated [14–19]. However, a customized SESAM with higher damage and two photon absorption thresholds is needed for higher average power. In contrast, the high-power KLM bulk laser is very promising. There are two ways currently to implement high-power pure KLM, either pumping with a powerful single-mode fiber laser or employing the dual-confocal cavity with an additional Kerr medium. The single-mode fiber laser has an excellent beam quality ($M^2 < 1.1$) so that its output beam can be focused to a very small spot with a long Rayleigh length. By pumping with a single-mode fiber laser, a few watts pure KLM lasers have been demonstrated operating at sub-40-fs pulses. In 2014, Sévillano *et al.* demonstrated a KLM Yb:CALGO laser with 1.1 W average power and 40 fs pulse duration [20]. By pumping Yb:CALYO crystal, 36 fs pulses with 2 W output power were realized by Tian *et al.* [21]. However, the single-mode fiber laser is not only expensive but also power limited. The dual-confocal cavity allows us to separate the gain medium and Kerr medium. Combining a big beam size in the gain medium and a small beam size in the Kerr medium, a high-power multi-mode laser diode (LD) can be used as the pump to obtain both high average power and strong Kerr-lens effect. The first KLM Yb-doped bulk laser based on this configuration was reported in 2015 [22], which generated 135 fs pulses with an output power of 1.85 W. Then shorter pulse duration of 68 fs was delivered by Yb:CALYO crystal with 1.5 W average power [23]. Soon after that, 4 W output power with 73 fs pulse duration was reported by the Yb:KGW crystal [24], and 6.2 W output power with 59 fs pulse duration was obtained from the KLM Yb:CALYO bulk laser [25]. However, the potential in high average power of this method is yet fully developed.

In this Letter, we demonstrated the generation of more than 10 W average power from a KLM Yb-bulk laser at 81 MHz. The long-term power stability is better than 0.3% (root mean

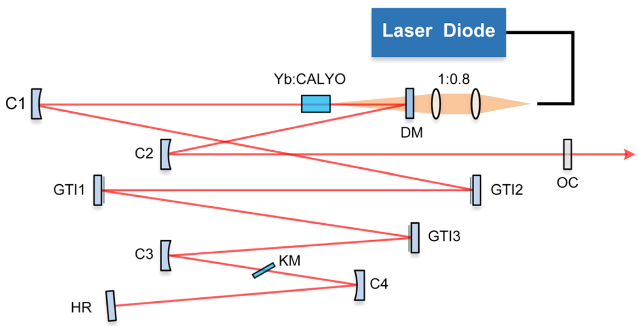

Fig. 1. Schematic of the high-power Yb:CALYO laser. DM, dichroic mirror; C1 and C2, concave mirrors with RoC of 300 mm; C3 and C4, concave mirrors with RoC of 100 mm; GTI1, GTI2, and GTI3, Gires–Tournois interferometer mirrors; KM, 2 mm CaF_2 plate as Kerr medium; HR, highly reflective mirrors; OC, 20% output coupler.

square, RMS) in 1 h. Thanks to the excellent optical properties of Yb:CALYO crystal and fine dispersion management, the pulse duration is less than 100 fs, resulting in a peak power of 1.14 MW. To our best knowledge, this is the highest average output power from a KLM bulk laser generating sub-100-fs pulses. The study of the dual-confocal cavity in terms of the Kerr sensitivity and pump-laser mode matching are also carried out.

The layout of the high-power KLM laser cavity is shown in Fig. 1. The pump source used for the experiment was a 50 W fiber-coupled unpolarized laser diode emitting at 976 nm (105 μm core diameter, 0.15 NA, $M^2 \approx 25$). After a commercial 1:0.8 couple system, the pump beam was reimaged into a $3 \times 3 \times 6$ mm c-cut Yb:CALYO crystal with 5 at. % doping, forming a beam radius around 52×54 μm (measured) at the focal plane. Without laser operation, over 91% of the pump power was absorbed due to the long crystal length and the high doping level. A 2-mm-thick CaF_2 plate acting as the Kerr medium was placed in the cavity at the Brewster-angle. In addition to providing Kerr nonlinearity and self-phase modulation (SPM), it also maintained the linear polarization and compensated for the astigmatism from the concave mirrors. The concave mirrors C1 and C2 provided a loose focusing in the gain medium (radius of curvature RoC = 300 mm), while C3 and C4 formed a tight focusing in the Kerr medium (radius of curvature RoC = 100 mm). The separation of C1 and C2 was fixed at 300 mm, and the gain crystal was positioned in the middle of them. Three Gires–Tournois interferometer (GTI) mirrors (Layertec GmbH) were used to introduce negative group delay dispersion (GDD) of $-5800\ fs^2$ per round trip in the cavity, which balanced the positive GDD ($+1268\ fs^2$) from the intracavity dispersion medium and SPM. To efficiently suppress the low-intensity background and extract high average power from the cavity, an output coupler (OC) with transmission of 20% was used in this work. This cavity was compact with a total length close to 1.85 m, corresponding to a repetition rate of 81 MHz.

When the cavity was set up and the continuous-wave (CW) laser started to oscillate, the optimization of the spatial matching between the pump and cavity modes was the first thing we did. First, the pitch of the end mirror and OC were adjusted to make the laser in the fundamental mode. Next, we changed the laser mode size in the gain crystal to fit the pump by moving the position of C4 along the light path. In the lower edge of the

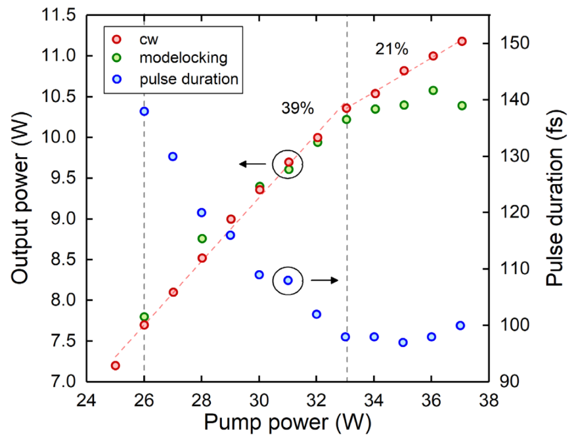

Fig. 2. Average output power and pulse duration as a function of the pump power. The red circles refer to the power of CW laser, while the green circles are the ML laser. The pulse duration is indicated by blue circles. Red dashed line from 25 to 33 W has a slope of 39% and 21% from 33 to 37 W. The left gray dashed line represents the start power for mode-locking, and the right gray dashed line recorded the pump power where the pulse duration and the ML power started to saturate.

stable region, we obtained a high slope efficiency of 39% in CW operation. But it decreased to 21% when the pump power was higher than 33 W because of the pump-saturation effects [26], as shown in Fig. 2. In order to avoid the damage of crystal, the maximum pump power was limited to 40 W.

As shown in Fig. 2, mode-locking operation can be initiated with the pump power of 26 W by a fast moving OC on the translation stage. The average output power at this point was 7.8 W, and the pulse duration was 138 fs. As the pump power increased to 33 W, the mode-locking power ramped up to 10.2 W. Because of the raise of the intracavity power density, the pulse duration decreased to 98 fs. As the pump power continued to increase, realignment of the laser cavity was needed for mode-locking, so that the average output power of the mode-locked (ML) laser did not increase and the pulse duration did not get shorter accordingly. This was because of the saturation of self-amplitude modulation (SAM) [27], where multiple pulses were likely to occur. Replacing folding mirrors of C3 and C4 to bigger RoC ones to enlarge the mode size on the Kerr medium may improve this situation [4].

The spectrum of the ML laser was characterized with an optical spectrum analyzer (AvaSpec-ULS4096CL-EVO) with a resolution of 0.6 nm, as shown in Fig. 3(a). A full width at half-maximum (FWHM) bandwidth of 12 nm at a center wavelength of 1050 nm was obtained. The $sech^2$-fit pulse duration of 98 fs was measured by a commercial intensity autocorrelator (APE PulseCheck USB) [Fig. 3(b)]. The autocorrelation trace measured in 50 ps delay span as inserted in Fig. 3(b) indicates that it was not operating in multi-pulse regime. The corresponding time-bandwidth product was 0.32, which is close to the Fourier transform limit assuming the $sech^2$ pulse shape (0.315). We recorded the pulse train by a 500 MHz bandwidth oscilloscope as shown in Fig. 4. There was neither *Q*-switched mode-locking nor multi-pulses observed.

In order to claim the stability of the 10 W KLM laser, the radio frequency (RF) spectrum was measured by a commercial RF spectrum analyzer (Agilent 4407B). Figure 5(a) shows the fundamental beat note at 81 MHz with a signal-to-noise

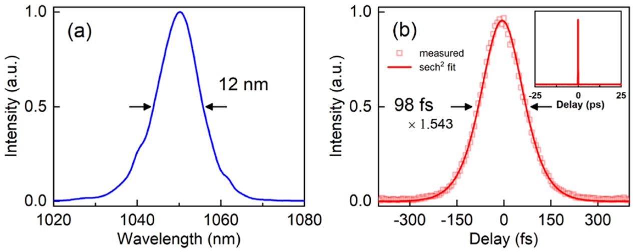

Fig. 3. (a) Optical spectrum of the 98 fs pulses at a pump power of 33 W. (b) The corresponding intensity autocorrelation trace with sech2-fit in the red curve and measured data in red squares. Inset, autocorrelation trace measured in a 50 ps delay span.

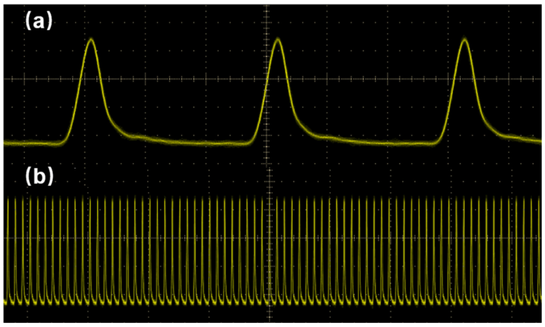

Fig. 4. Sampling oscilloscope traces of 98 fs pulses at repetition rate of 81 MHz in the time scale of (a) 4 ns/div and (b) 100 ns/div.

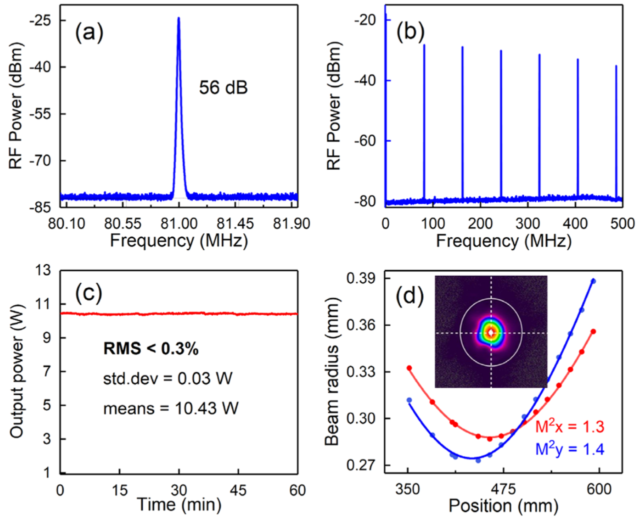

Fig. 5. (a) Radio frequency spectrum of the fundamental repetition rate frequency at 81 MHz with a RBW of 10 kHz. (b) The harmonics within 500 MHz span with 10 kHz RBW. (c) Average power stability during 60 min. (d) Beam quality of the laser beam with max average power of 10.4 W.

ratio of 56 dB with a resolution bandwidth (RBW) of 10 kHz. Figure 5(b) shows the harmonics in 500 MHz frequency range with 10 kHz RBW. No obvious side peaks around the several harmonics were observed, which indicated that the mode-locking is very clean. We also measured the long-term stability of the output power shown in Fig. 5(c). Once mode-locking was started, it was stable longer than 6 h, and the RMS in 1 h was smaller than 0.3% at average power of 10.4 W. At last, we tested the M^2 factors using a commercial M^2 factor meter (BSQ-SP920), which were 1.3 and 1.4 in the horizontal and vertical directions, as shown in Fig. 5(d).

The soft aperture technique was used in the experiment for KLM as it introduces less loss than the hard aperture [28]. It is important to note that the soft aperture KLM in this kind of cavity behaves differently from that of the conventional one. In the conventional KLM cavity, the Kerr-lens effect and soft aperture effect happen in the same place (gain medium), while in the dual-confocal cavity, they happen in the Kerr medium and the gain medium, respectively, which means that the Kerr-lens effect can be optimized independently meanwhile keeping the well overlap between the pump and the ML laser. For deeper understanding of this dual-confocal cavity, the Kerr sensitivity and pump-laser mode matching are discussed.

The Kerr sensitivity parameter δ is widely used to quantitatively evaluate the KLM operation [29–31], defined as follows:

$$\delta = \frac{-1}{\omega} \frac{d\omega}{dP},$$

where ω means the mode radius at the aperture plane and P is the intracavity peak power. δ represents the relative spot size variation due to the self-focusing effect. When it is negative, the mode size would be reduced for the ML laser to the CW laser in the aperture plane so that the system can favor the pulsed regime over the CW one with a soft aperture. Here we used the analytical solution of δ presented by Magni *et al.* [32]. As shown in Fig. 6(a), the stable ranges were determined by the distance of mirrors C3 and C4, which was around 2.5 mm between the two horizontal black dotted lines (from 100.6 to 103.1 mm). The horizontal coordinate represents the KM position. The value of δ was shown in the colors of red (>0) and blue (<0). According to Cerullo *et al.*, the KLM could be easily started and maintained for hours if $\delta < -0.5$ [33]. So in this dual-confocal cavity, we find that there were two strong Kerr sensitivity regions in the upper and lower edges of the stable region where 100.6 mm $<$ C3−C4 $<$ 101.2 mm, 48.5 mm $<$ C3−KM $<$ 50 mm and 102.5 mm $<$ C3−C4 $<$ 103.1 mm, 51.1 mm $<$ C3−KM $<$ 52.5 mm. But in the experiment, we could only start the KLM in the lower edge of the stable region. And the most stable Kerr-lens mode-locking operation was obtained where the separation between C3 and C4 was 101 mm and the corresponding distance between the C3 and CaF_2 plate was 49.5 mm. Thus, the CaF_2 was a little away from the focus point, and the laser mode radius in CaF_2 plate was estimated to be 20 µm. To explain this phenomenon, the mode match ratio of the CW laser and pump was calculated, as shown in Fig. 6(b). The vertical coordinate represents stability zones, and the horizontal coordinate equals the CW laser mode (in the middle of the gain crystal) divided by the pump radius. For a suitable soft aperture KLM, the fundamental CW laser mode should be a little bit bigger than the pump. However, in the upper stable region, the laser mode becomes too big, and it not only influences the start of KLM but also reduces laser efficiency because of the reabsorption effect in the unpumped regions of the gain crystal. Perfect mode match was found in the lower edge of the stable region, where soft aperture KLM could be worked.

The above analysis about the Kerr sensitivity and pump-laser mode indicates a solution to further scale the average power in this dual-confocal cavity. First, a higher ratio couple system

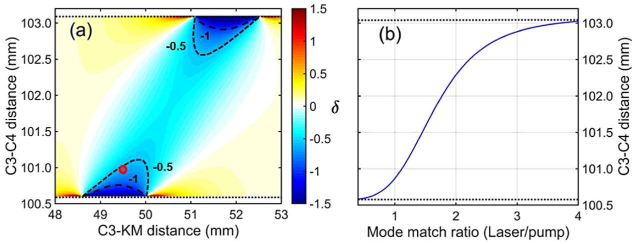

Fig. 6. (a) Kerr sensitivity in gain crystal as a function of the position of KM and the distance between C3 and C4. The red circle marks the operation point of the stable Kerr-lens mode-locking. (b) Mode match ratio at a pump radius of 50 μm, which is also shown versus the separation distance of C3 and C4. The horizontal black dotted lines limit the stable region.

Table 1. Overview of the State-of-the-art of High-power KLM Yb-doped Oscillator with Sub-100-fs Pulses[a]

Type	Gain Crystal	τ	P_{ave}	η_{o-o}	Reference
TDL	$Yb:Lu_2O_3$	35 fs	1.6 W	5.8%	[6]
TDL	$Yb:Lu_2O_3$	95 fs	21.1 W	16.2%	[8]
Bulk	$Yb:YVO_4$	80 fs	1 W	28.5%	[34]
Bulk	Yb:YSO	95 fs	2 W	27%	[11]
Bulk	$Yb:CaF_2$	68 fs	2.3 W	33%	[35]
Bulk	Yb:KGW	73 fs	4 W	18%	[24]
Bulk	Yb:CALGO	40 fs	1.1 W	12%	[20]
Bulk	Yb:CALYO	68 fs	1.5 W	6%	[23]
Bulk	Yb:CALYO	36 fs	2 W	31%	[21]
Bulk	Yb:CALYO	59 fs	6.2 W	–	[25]
Bulk	Yb:CALYO	98 fs	10.4 W	30%	This work

[a] τ, pulse duration; P_{ave}, average output power; η_{o-o}, optical-to-optical efficiency.

could be used to expand the pump radius in the gain medium. So higher pump power can be used before encountering the pump-saturation effects. Second, the operation area of mode-locking is then moved to the upper edge of stable region, where the laser mode becomes much bigger and matches the pump better. Therefore, a suitable soft aperture effect could be formed for the high-power KLM laser.

In summary, we have demonstrated the generation of 98 fs pulses with an average power of 10.4 W at a repetition rate of 81 MHz directly from the KLM Yb:CALYO oscillator, corresponding to the pulse energy of 0.12 μJ and the peak power of 1.14 MW. The final average output power is much higher than any other KLM bulk laser as summarized in Table 1. The optical-to-optical efficiency was 30% using 20% OC. The power stability was better than 0.3% (RMS) over 1 h with a beam quality of 1.3 and 1.4 in the horizontal and vertical directions.

In the next step, scaling of the mode radius of the pump and laser would be taken by the use of a large coupled system and adjusting the mirror distance. The dual-crystal geometry would be able to generate higher average power when mode-locking in the upper edge of the stable region.

Funding. National Key Basic Research Program of China (2017YFB0405202); National Natural Science Foundation of China (11774277, 61705174); Fundamental Research Funds for the Central Universities (JB190501, ZD2006); Natural Science Basic Research Program of Shaanxi Province (2019JCW-03) .

Disclosures. The authors declare no conflicts of interest.

REFERENCES

1. T. Südmeyer, S. V. Marchese, S. Hashimoto, C. R. E. Baer, G. Gingras, B. Witzel, and U. Keller, Nat. Photonics **2**, 599 (2008).
2. K. M. T. Ahmmed, C. Grambow, and A. Kietzig, Micromachines **5**, 1219 (2014).
3. C. J. Saraceno, F. Emaury, C. Schriber, A. Diebold, M. Hoffmann, M. Golling, T. Südmeyer, and U. Keller, IEEE J. Sel. Top. Quantum Electron. **1**, 1100318 (2015).
4. J. Brons, V. Pervak, E. Fedulova, D. Bauer, D. Sutter, V. Kalashnikov, A. Apolonskiy, O. Pronin, and F. Krausz, Opt. Lett. **39**, 6442 (2014).
5. F. Saltarelli, I. J. Graumann, L. Lang, D. Bauer, C. R. Phillips, and U. Keller, Opt. Express **27**, 31465 (2019).
6. C. Paradis, N. Modsching, V. J. Wittwer, B. Deppe, C. Kränkel, and T. Südmeyer, Opt. Express **25**, 14918 (2017).
7. A. Diebold, F. Emaury, C. Schriber, M. Golling, C. J. Saraceno, T. Südmeyer, and U. Keller, Opt. Lett. **38**, 3842 (2013).
8. N. Modsching, J. Drs, J. Fischer, C. Paradis, F. Labaye, M. Gaponenko, C. Kränkel, V. J. Wittwer, and T. Südmeyer, Opt. Express **27**, 16111 (2019).
9. N. V. Kuleshov, A. A. Lagatsky, A. V. Podlipensky, V. P. Mikhailov, and G. Huber, Opt. Lett. **22**, 1317 (1997).
10. M. Siebold, S. Bock, U. Schramm, B. Xu, J. L. Doualan, P. Camy, and R. Moncorgé, Appl. Phys. B **97**, 327 (2009).
11. W. Tian, J. Zhu, Y. Peng, Z. Wang, L. Zheng, L. Su, J. Xu, and Z. Wei, Opt. Express **26**, 5962 (2018).
12. J. Petit, P. Goldner, and B. Viana, Opt. Lett. **30**, 1345 (2005).
13. D. Li, X. Xu, H. Zhu, X. Chen, W. Tan, J. Zhang, D. Tang, J. Ma, F. Wu, C. Xia, and J. Xu, J. Opt. Soc. Am. B **28**, 1650 (2011).
14. A. Greborio, A. Guandalini, and J. Aus der Au, Proc. SPIE **8235**, 823511 (2012).
15. H. Zhao and A. Major, Opt. Express **22**, 30425 (2014).
16. F. Pirzio, S. D. D. D. Cafiso, M. Kemnitzer, F. Kienle, A. Guandalini, J. A. D. Au, and A. Agnesi, J. Opt. Soc. Am. B **32**, 2321 (2015).
17. R. Akbari, H. Zhao, K. A. Fedorova, E. U. Rafailov, and A. Major, Opt. Lett. **41**, 3771 (2016).
18. R. Akbari, K. A. Fedorova, E. U. Rafailov, and A. Major, Appl. Phys. B **123**, 123 (2017).
19. S. Manjooran and A. Major, Opt. Lett. **43**, 2324 (2018).
20. P. Sévillano, P. Georges, F. Druon, D. Descamps, and E. Cormier, Opt. Lett. **39**, 6001 (2014).
21. W. Tian, G. Wang, D. Zhang, J. Zhu, Z. Wang, X. Xu, J. Xu, and Z. Wei, High Power Laser Sci. Eng. **7**, e64 (2019).
22. I. Tomohiro, A. A. Eilanlou, N. Yasuo, F. Yoshihiko, I. Tomohiro, S. Tetsumi, K. Fumihiko, K.-G. Makoto, and M. Katsumi, Jpn. J. Appl. Phys. **54**, 072703 (2015).
23. W. Tian, Y. Peng, Z. Zhang, Z. Yu, J. Zhu, X. Xu, and Z. Wei, Photon. Res. **6**, 127 (2018).
24. X. Meng, L. Chong, Q. Liu, X. Zhang, Y. Li, X. Xi, and B. Zhao, Appl. Phys. B **125**, 166 (2019).
25. W. Tian, C. Yu, J. Zhu, D. Zhang, Z. Wei, X. Xu, and J. Xu, Opt. Express **27**, 21448 (2019).
26. F. Sanchez, M. Brunel, and K. Aït-Ameur, J. Opt. Soc. Am. B **15**, 2390 (1998).
27. M. A. Larotonda, Opt. Commun. **228**, 381 (2003).
28. L. Xu, G. Tempea, A. Poppe, M. Lenzner, C. Spielmann, F. Krausz, A. Stingl, and K. Ferencz, Appl. Phys. B **65**, 151 (1997).
29. R. Akbari and A. Major, Laser Phys. Lett. **15**, 085001 (2018).
30. P. Xia, K.-G. Makoto, and Y. Kosuke, Jpn. J. Appl. Phys. **59**, 062002 (2020).
31. S. Kitajima, A. Shirakawa, H. Yagi, and T. Yanagitani, Opt. Lett. **43**, 5451 (2018).
32. V. Magni, G. Cerullo, and S. De Silvestri, Opt. Commun. **101**, 365 (1993).
33. G. Cerullo, S. De Silvestri, V. Magni, and L. Pallaro, Opt. Lett. **19**, 807 (1994).
34. F. Bain, A. Lagatsky, C. Brown, and W. Sibbett, Proc. SPIE **6871**, 68712L (2008).
35. G. Machinet, P. Sevillano, F. Guichard, R. Dubrasquet, P. Camy, J.-L. Doualan, R. Moncorgé, P. Georges, F. Druon, D. Descamps, and E. Cormier, Opt. Lett. **38**, 4008 (2013).